Electronic Supplementary Material (ESI) for Journal of Materials Chemistry C.

Supporting Information

High mobility n-type organic semiconductors with tunable exciton dynamics toward photo-stable and photo-sensitive transistors

Li Yu,[a] Yongxu Hu,[a] Jie Li,[ac] Zhongwu Wang,[a] Haoquan Zhang,[a] Yinan Huang,[a] Yunpeng Lou,[a] Yajing Sun,[a] Xueying Lu,[a] Huapeng Liu,[a] Yingshuang Zheng,[a] Shuguang Wang,[a] Xiaosong Chen,[ac] Deyang Ji,[ac] Liqiang Li*[abc] and Wenping Hu[abc]

[a] Tianjin Key Laboratory of Molecular Optoelectronic Sciences, Department of Chemistry, Institute of Molecular Aggregation Science, Tianjin University, Tianjin 300072, China

[b] Joint School of National University of Singapore and Tianjin University, International Campus of Tianjin University, Binhai New City, Fuzhou 350207, China

[c] Haihe Laboratory of Sustainable Chemical Transformations, Tianjin 300192, China

Table of contents

1. General Information.....1

2. Synthesis.....2

3. Thermal properties.....3

4. Optical properties.....4

5. Cyclic voltammetry.....4

6. Computational studies.....5

7. Crystal structures.....5

8. Characterization of single crystal transistors.....7

9. NMR spectra.....14

10. HRMS.....15

11. References.....16

1. General Information

1.1 Materials and instruments

The starting materials and reagents employed were commercially available and used without any further purification. NMR spectra were recorded on a JEOL 600 MHz spectrometer (JNM-ECZ400S/L1). Chemical shift values (δ) are expressed in parts per million using residual solvent protons as internal standard (^{1}H NMR, δ(H) is 7.26 ppm for $CDCl_3$). High-resolution mass spectra (HRMS) were measured with MALDI-TOF/TOF Mass Spectrometer. Thermogravimetric analysis (TGA) was measured from 40 °C to 800 °C by Thermo Gravimetric Analyzer TG 209F3 of Netzsch in N_2. UV-vis absorption spectra were recorded on Shimadzu UV-2700 UV-vis spectrophotometer. Photoluminescence (PL) spectra were measured on a FLS1000 fluorescence spectrophotometer. The micro-PL spectra were measured by RENISHAW laser Raman spectrometer. Cyclic voltammetry (CV) was performed on AUTOLAB PGSTAT 302N electrochemical analyzer at a scan rate of 100 mV/s, PQ-4FP and PQ-4ClP were dissolved in dichloromethane (DCM) with 0.1 mol/L tetrabutylammonium hexafluorophosphate (Bu_4NPF_6) as supporting electrolyte. A glassy carbon electrode as a working electrode, a platinum wire was used as an auxiliary electrode, and Ag/AgCl was used as a pseudo-reference. Ferrocene/ferrocenium was used as an internal standard. X-ray diffractometer data was completed by MiniFlex600 (Rigaku). X-ray crystallography data were collected on a SuperNova double micro focal spot X-ray single-crystal Diffractometer. The single crystals of PQ-4FP and PQ-4ClP were prepared in the dichloromethane and toluene by slow solvent vapor-diffusion method. Energy-minimized models of PQ-4FP and PQ-4ClP were calculated using Gaussian 09W program at the B3LYP/6-31G(d, p) level of Density Function Theory (DFT). The transfer integrals, reorganization energies and the drift mobilities of these semiconductors were calculated by using Gaussian 09 program. The optimized structures of PQ-4FP and PQ-4ClP were obtained based on two-layer quantum mechanics/molecular mechanics (QM/MM) method with electronic embedding scheme in Gaussian 09 package.[1] One central molecule was set as higher layer, computed by PBE0 functional with 6-31G(d) basis set. The sufficient surrounding molecules were

set as lower layer, calculated by UFF molecular mechanics method.

1.2 Device fabrication and characterization

To improve the molecular stacking quality, the heavily n-doped Si/SiO_2 substrates (thickness of oxide layer was 300nm) were firstly treated with O_2 plasma (5 minutes, 50 W). Then the substrates and a drop of octadecyl-trichlorosilane (OTS) (5 μL) were heated in a vacuum oven at 120 °C for two hours. After cooling to room temperature, the substrates were ultrasonically cleaned with n-hexane, chloroform, isopropanol for 10 minutes, respectively, and dried with a flow of high-purity nitrogen. After modifying the substrates, the single crystals of the two compounds were then prepared by the physical vapor transport (PVT) method (high-purity N_2 as the carrier gas). High-quality ribbon single crystals (PQ-4FP) and hexagon single crystals (PQ-4ClP) were obtained at 240 °C and 40 sccm gas flow rate for 60 min. Finally, attaching gold strips on the single crystals as the source and drain electrodes to complete the fabrication of the single crystals organic field-effect transistors (SC-OFETs). The electrical performance of the devices was characterized by an Agilent B1500A semiconductor parameter analyzer in a nitrogen glove box. Xenon light source was used as the white light source. The photo-stable and photo-response tests were carried out under the irradiation of white light and fixed wavelength laser (385 nm).

To evaluate the performance of PQ-4ClP single crystal phototransistors, photosensitivity (P), responsivity (R), and detectivity (D^*) are calculated according to equations:

$$P = |I_{photo}\text{-}I_{dark}|/ I_{dark} \quad (1)$$

$$R = |I_{photo}\text{-}I_{dark}| / SP_i \quad (2)$$

$$D^* = RS^{1/2}/(2eI_{dark})^{1/2} \quad (3)$$

2. Synthesis

2.1. Synthesis of PQ-4FP

1,2,4,5-Benzenetetramine tetrahydrochloride (1.0 mmol, 0.284 g) was dissolved in acetic acid glacial (8 mL), followed by adding 1,2-Bis(4-fluorophenyl)-1,2-ethanedione (2.0 mmol, 0.492 g), After reflux for 24 h, the reaction mixture was cooled to room

temperature, and the resulting precipitate was collected by filtration and then washed with ultrapure water and anhydrous alcohol until the filtrate was colorless. The yellowish-green residue was purified by column chromatography on silica gel with ethyl acetate/petroleum ether (1/10, V/V) as eluent to give product. Yield of PQ-4FP: 64.1 % (357.8 mg, 0.64 mmol), bright yellow solid. PQ-4FP ^{1}H NMR (600 MHz, Chloroform-*d*) δ (ppm): 8.97 (s, 2H), 7.60 (s, 8H), 7.10 (s, 8H). HRMS-EI^{+} (m/z): [M^{+}+H] calculated for $C_{34}H_{18}F_4N_4$: 559.1540, found: 559.1532.

2.2. Synthesis of PQ-4ClP

1,2,4,5-Benzenetetramine tetrahydrochloride (1.0 mmol, 0.284 g) was dissolved in acetic acid glacial (8 mL), followed by adding 1,2-Bis(4-chlorophenyl)ethane-1,2-dione (2.0 mmol, 0.558 g), After reflux for 24 h, the reaction mixture was cooled to room temperature, and the resulting precipitate was collected by filtration and then washed with ultrapure water and anhydrous alcohol until the filtrate was colorless. The yellowish-green residue was purified by column chromatography on silica gel with ethyl acetate/petroleum ether (1/2, V/V) as eluent to give product. Yield of PQ-4ClP: 57.3 % (357.6 mg, 0.57 mmol), yellow solid. PQ-4ClP ^{1}H NMR (600 MHz, Chloroform-*d*) δ (ppm): 8.97 (s, 2H), 7.56 (s, 8H), 7.39 (s, 8H). HRMS-EI^{+} (m/z): [M^{+}+H] calculated for $C_{34}H_{18}F_4N_4$: 625.0334, found: 625.0317.

3. Thermal properties

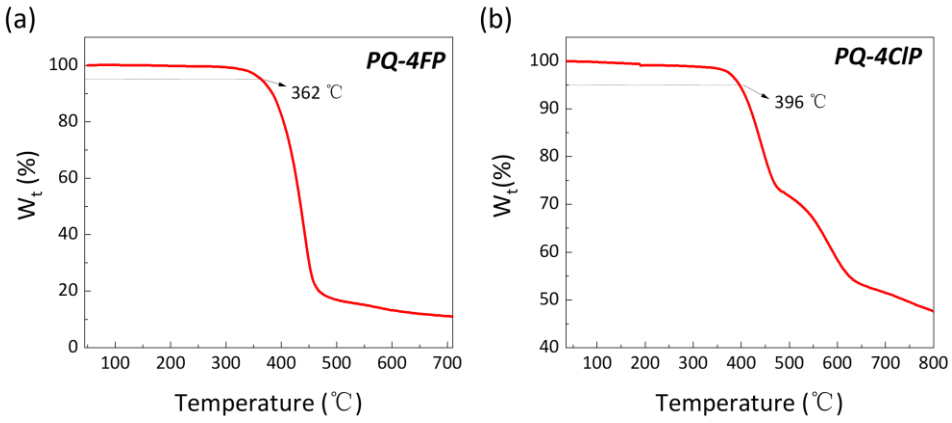

Fig. S1 TGA of a) PQ-4FP, b) PQ-4ClP in N_2.

4. Optical properties

Table S1 Summary of fluorescence data of PQ-4FP and PQ-4ClP.

Compound	$\lambda_{em.\ max}$ (nm)		Quantum yield (ΦF)		τ (ns)
	solution	crystal	solution	crystal	
PQ-4FP	460	490	3.5	5.7	0.56
PQ-4ClP	463	496	4.6	7.8	0.59

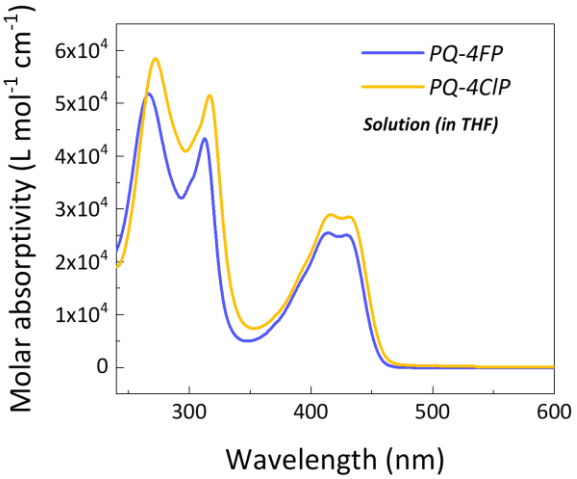

Fig. S2 Molar absorptivity of PQ-4FP and PQ-4ClP.

5. Cyclic voltammetry

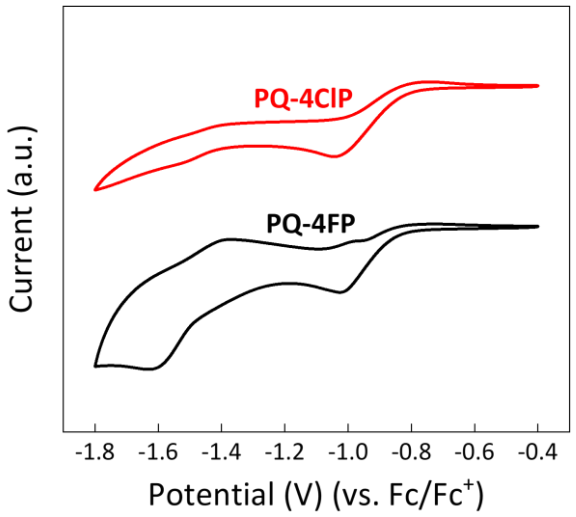

Fig. S3 Cyclic voltammograms of PQ-4FP and PQ-4ClP recorded in DCM with ferrocene/ferrocenium as the internal standard.

6. Computational studies

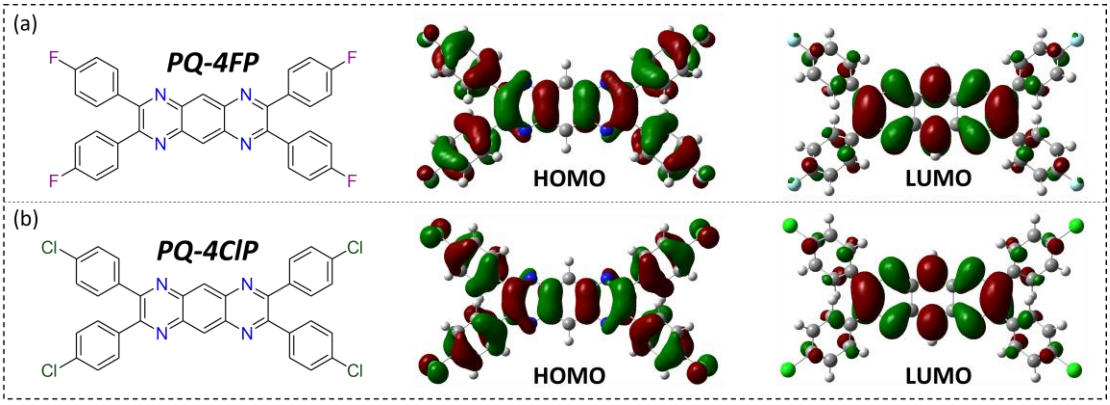

Fig. S4 Molecular frontier orbitals of PQ-4FP and PQ-4ClP.

7. Crystal structures

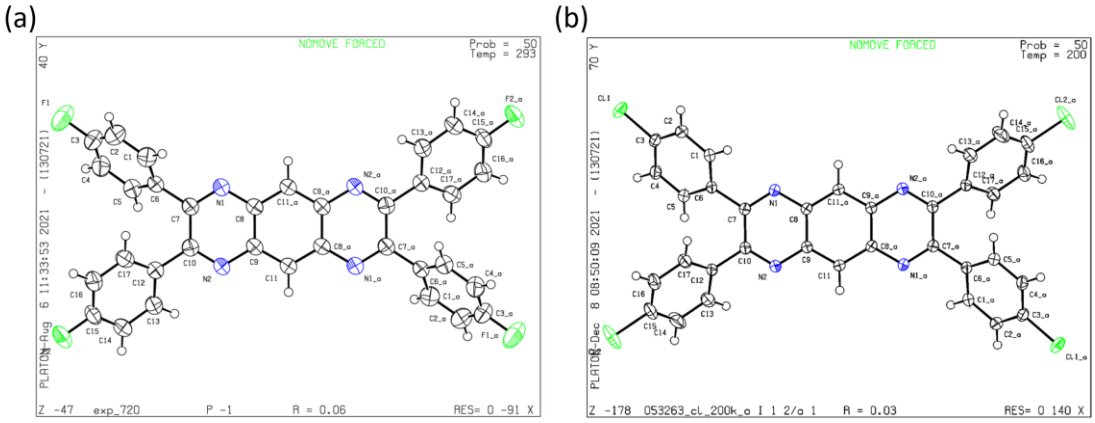

Fig. S5 X-ray crystallographic data of a) PQ-4FP and b) PQ-4ClP.

Table S2 The π-π distances, displacements of π-stacking and volume per molecule in PQ-4FP and PQ-4ClP.

Compound	π-π distance (Å)	Displacements of π-stacking (Å)		Volume per molecule (Å^3)
		along the short axis	along the long axis	
PQ-4FP	3.612	3.586	3.09	645.372
PQ-4ClP	3.875	/	/	471.932

Table S3 Summary of crystallographic data of PQ-4FP and PQ-4ClP.

Compound	Space Group	Unit Cell Length	Unit Cell Angles (deg)	Cell Volume ($Å^3$)
PQ-4FP	Pī	a=5.8574	α=84.831	645.372
		b=7.9358	β=88.443	
		c=14.6368	γ=72.261	
PQ-4ClP	I 2/a	a=8.2699	α=90	2831.59
		b=11.0285	β=97.033	
		c=31.2819	γ=90	

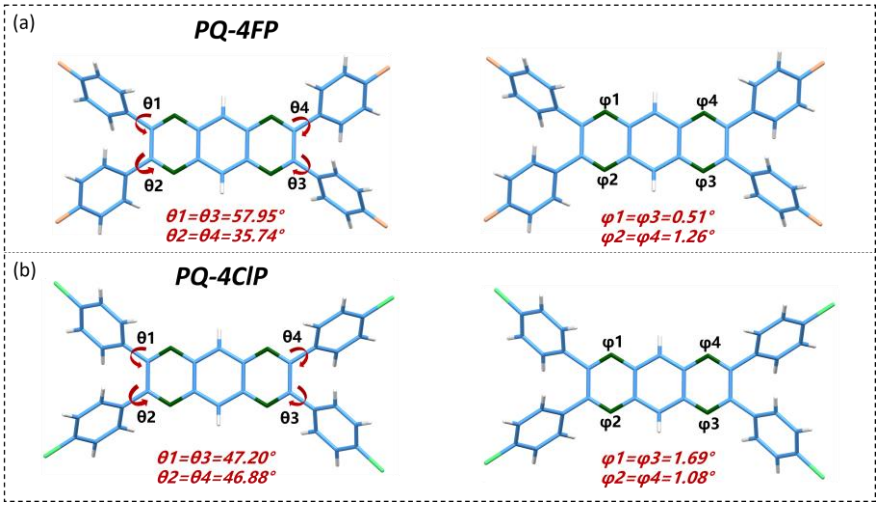

Fig. S6 Molecular conformation of a) PQ-4FP and b) PQ-4ClP.

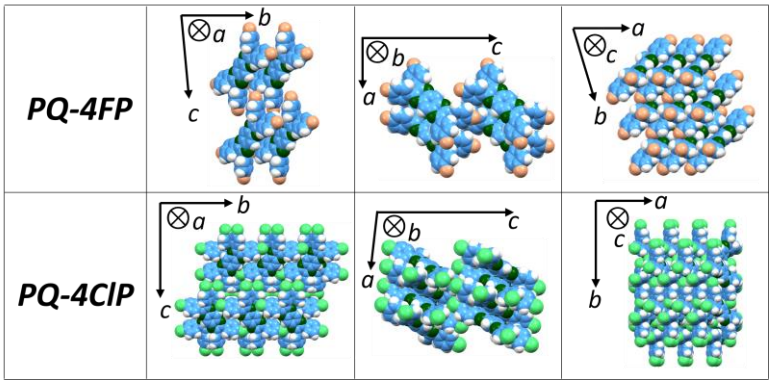

Fig. S7 The packing of PQ-4FP and PQ-4ClP molecules in the single crystals along different axis.

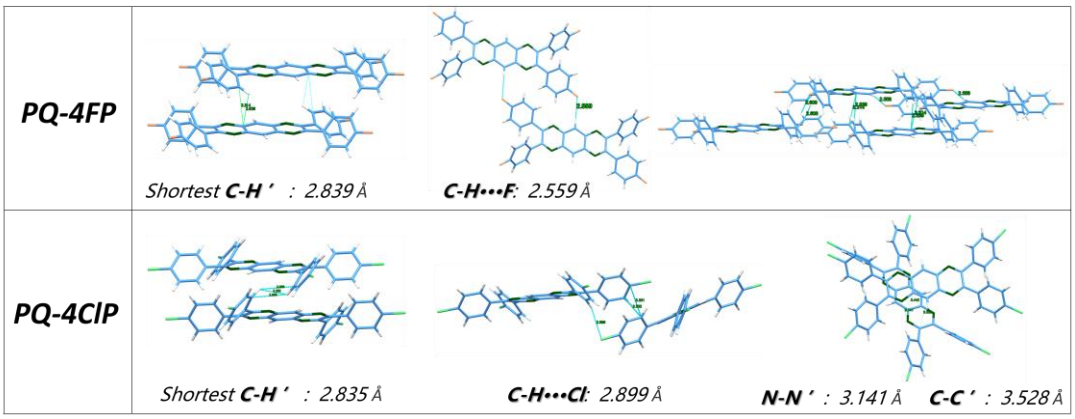

Fig. S8 Intermolecular short distances of PQ-4FP and PQ-4ClP in the crystals.

8. Characterization of single crystal transistors

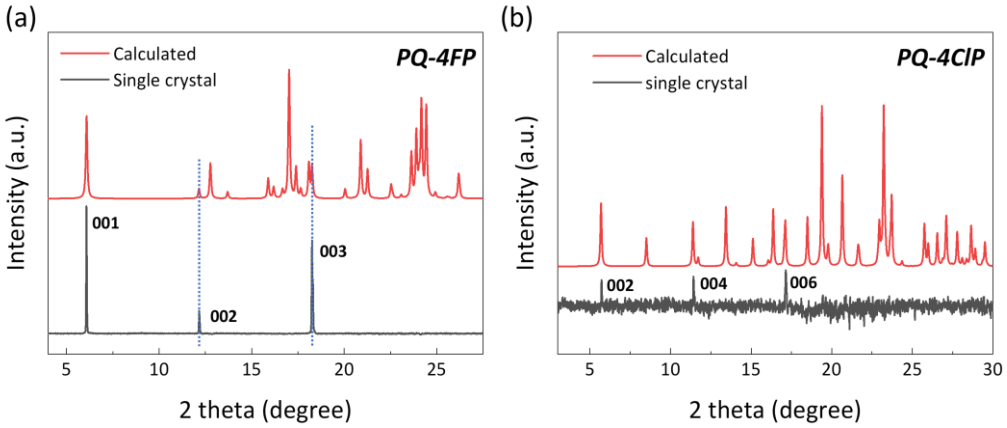

Fig. S9 The XRD patterns of a) PQ-4FP and b) PQ-4ClP (single crystals grown on silicon wafer and calculated from single crystal structures).

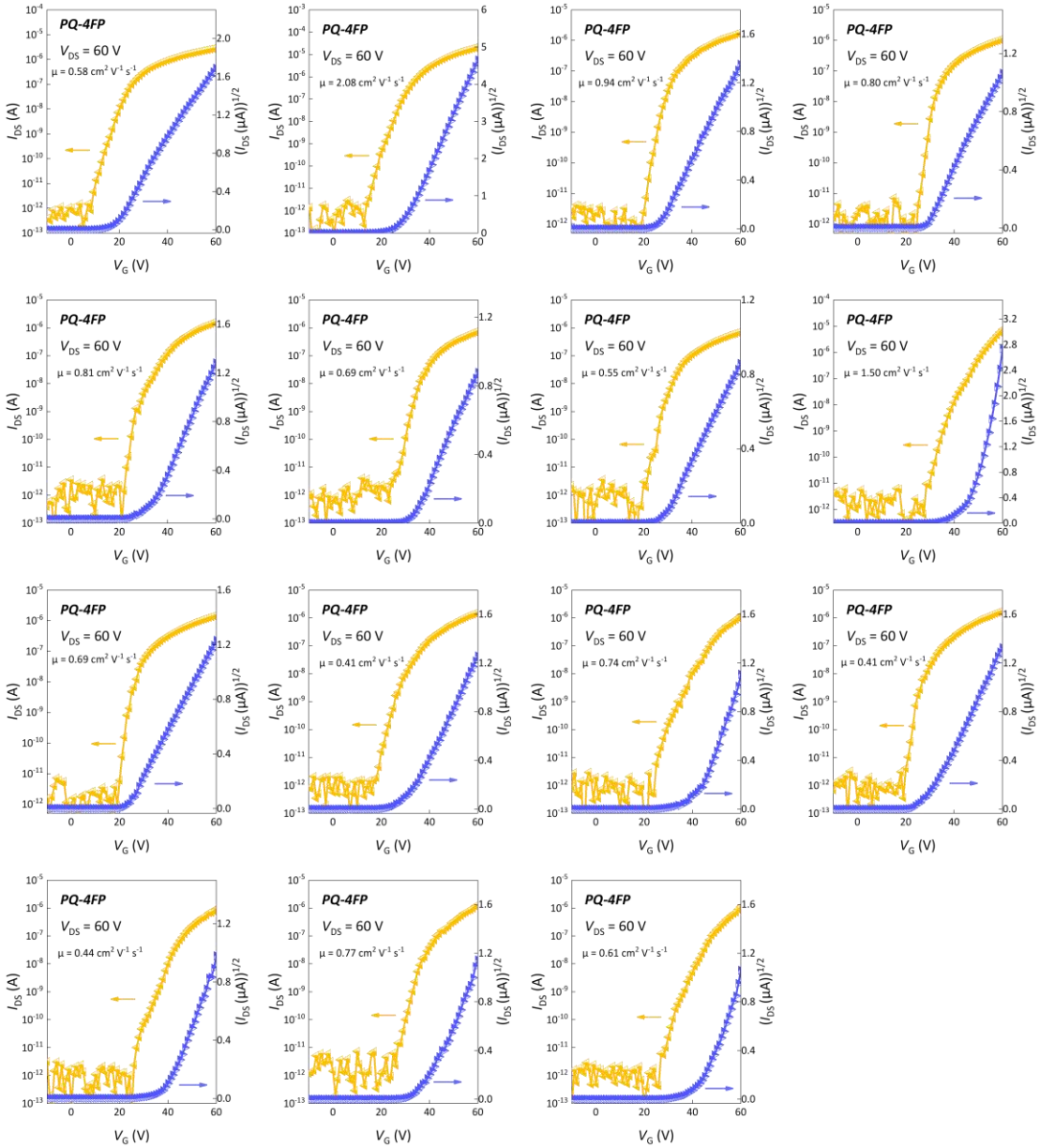

Fig. S10 Transfer curves of SC-OFETs based on PQ-4FP.

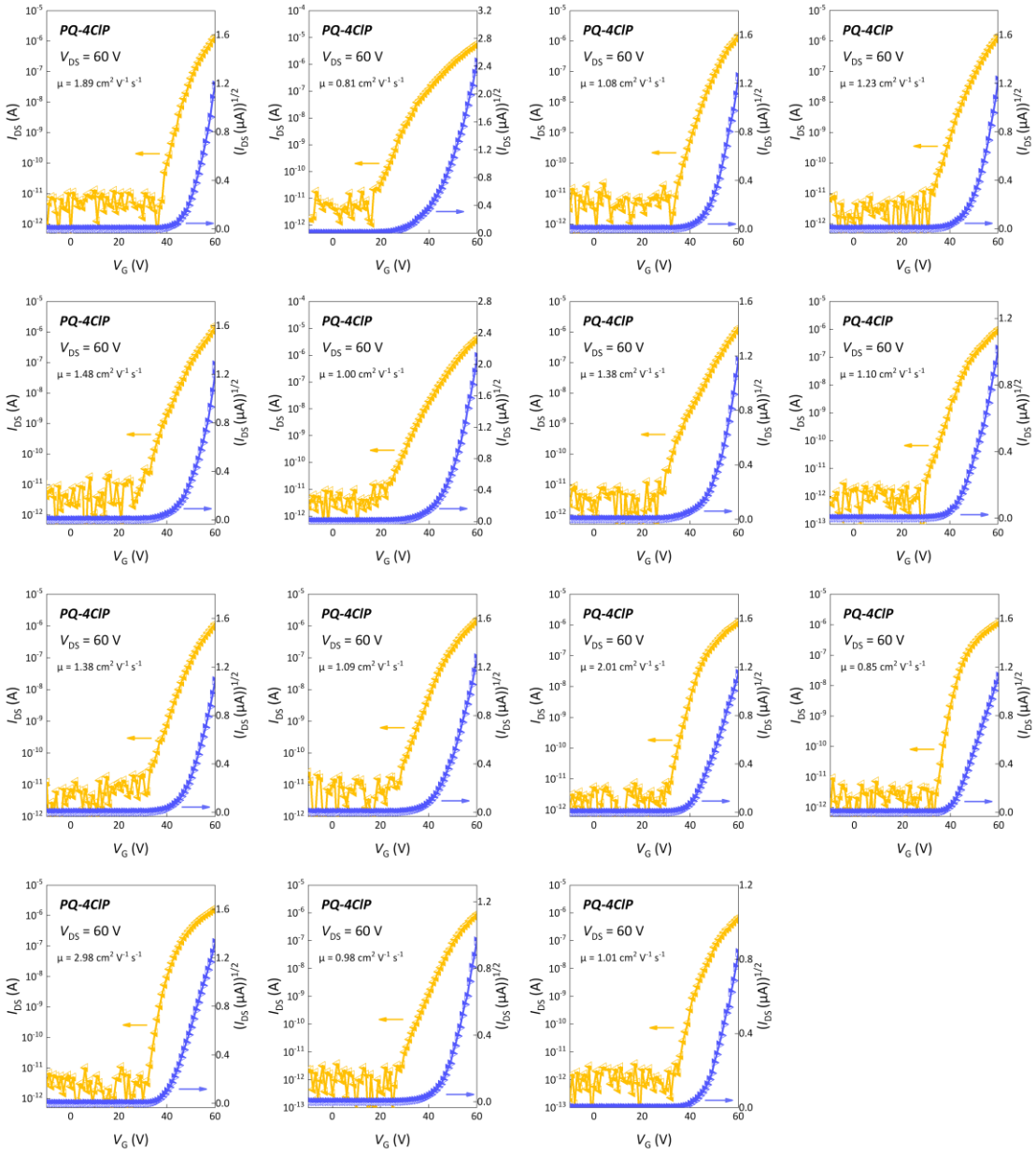

Fig. S11 Transfer curves of SC-OFETs based on PQ-4ClP.

Table S4 Electronic properties of SC-OFETs of PQ-4FP and PQ-4ClP.

Compound	$\mu_{e,\,max}$ ($cm^2\ V^{-1}\ s^{-1}$)	$\mu_{ave.}$ ($cm^2\ V^{-1}\ s^{-1}$)	I_{on}/I_{off}
PQ-4FP	2.08	0.81	10^6-10^7
PQ-4ClP	2.98	1.35	10^5-10^7

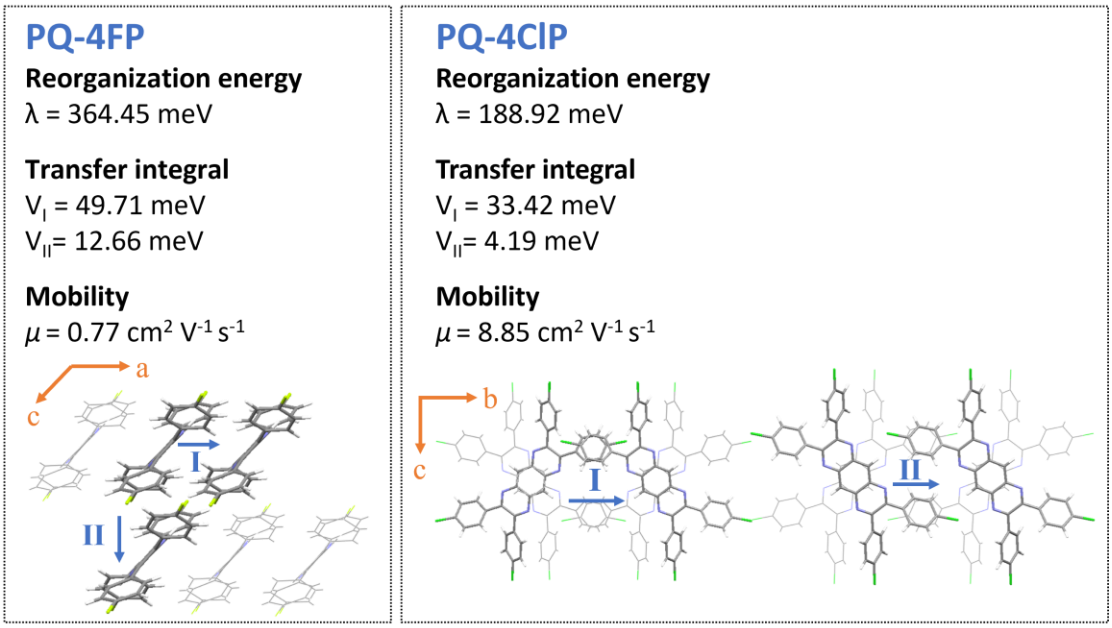

Fig. S12 The reorganization energies, transfer integrals and the drift mobilities of PQ-4FP and PQ-4ClP.

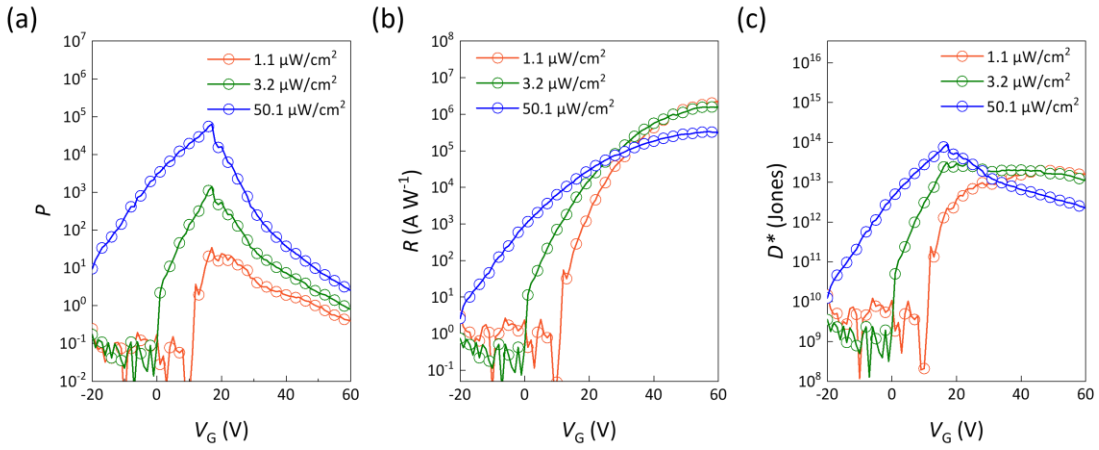

Fig. S13 The effect of V_G modulation on PQ-4ClP device performance under different light power density at 385 nm: a) *P*, b) *R* and c) *D**.

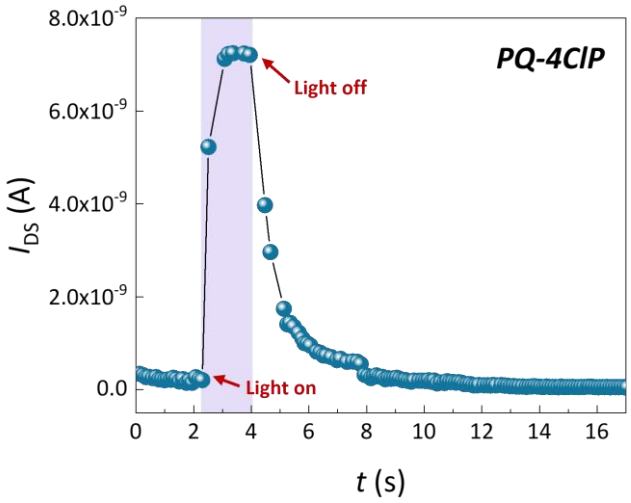

Fig. S14 I_{DS}-t curves of SC-OFETs based on PQ-4ClP measured with V_{DS} = 60 V and V_G = 20 V in nitrogen glove box, wherein the purple shadow represents the light (385 nm) illumination period.

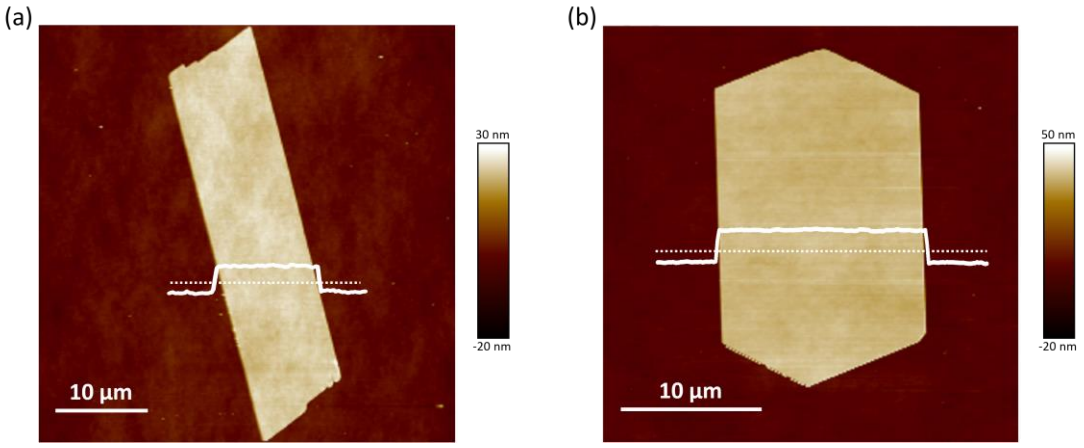

Fig. S15 AFM images of a) PQ-4FP and b) PQ-4Cl. Inset: the height changes of the single crystals.

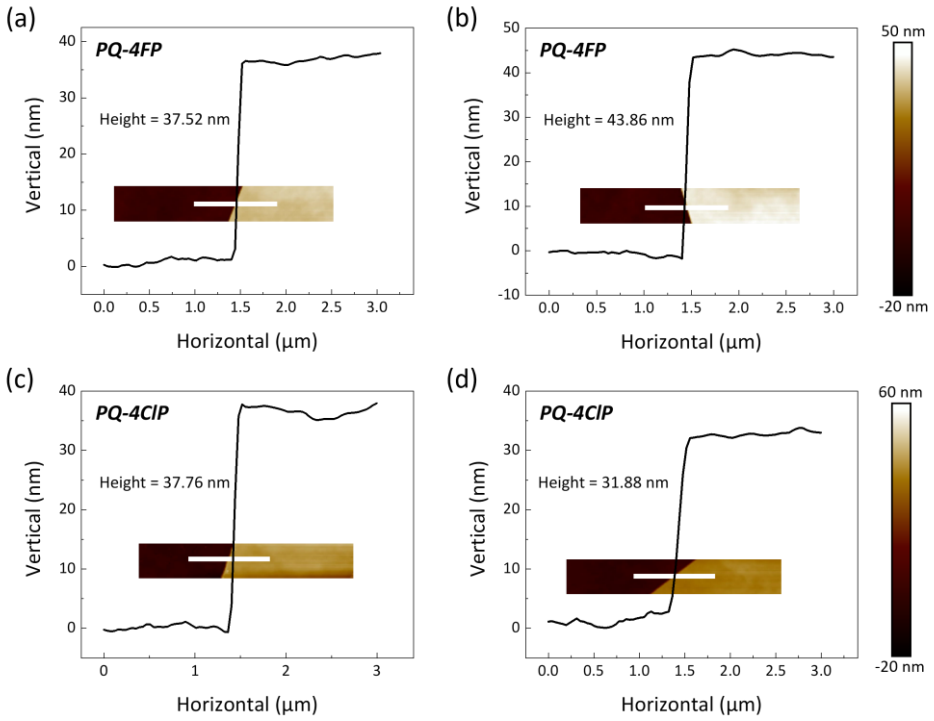

Fig. S16 The height maps of a,b) PQ-4FP, c,d) PQ-4ClP single crystals. (Inset: the AFM images of single crystals. Scale bar: 3 μm.)

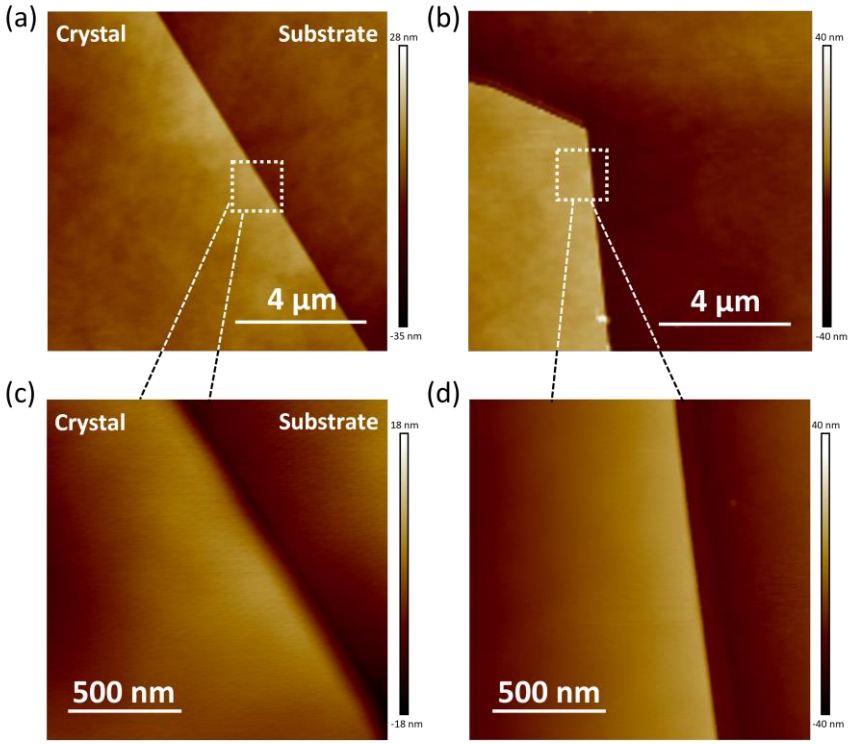

Fig. S17 AFM images of a,c) PQ-4FP, b,d) PQ-4ClP single crystals.

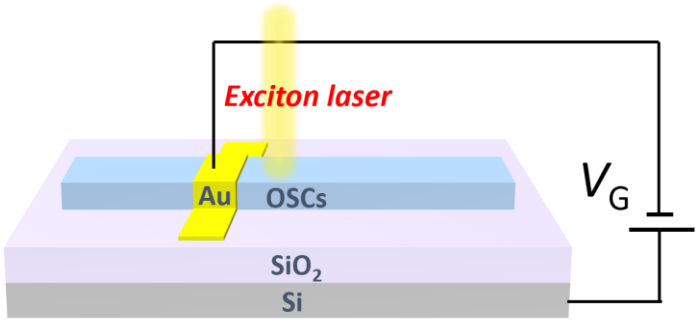

Fig. S18 Schematic diagram of Au/single crystal/dielectric/Si structure in in-situ micro-photoluminescence spectroscopy measurement.

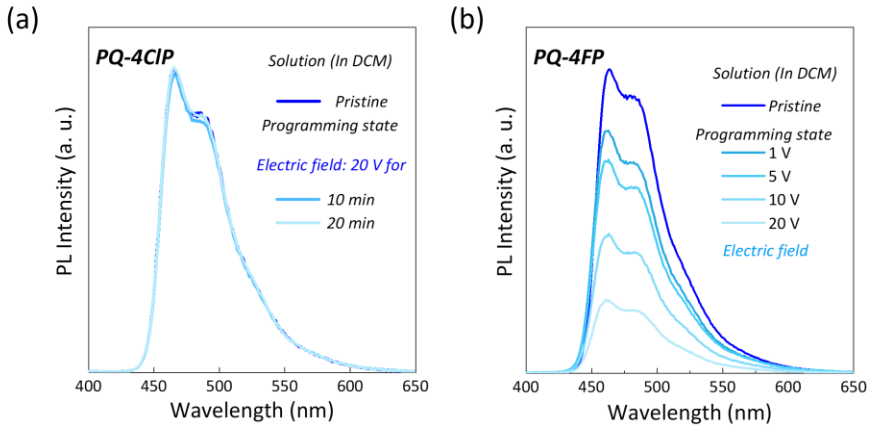

Fig. S19 Steady-state PL spectra of a) PQ-4ClP and b) PQ-4FP solution under electric field.

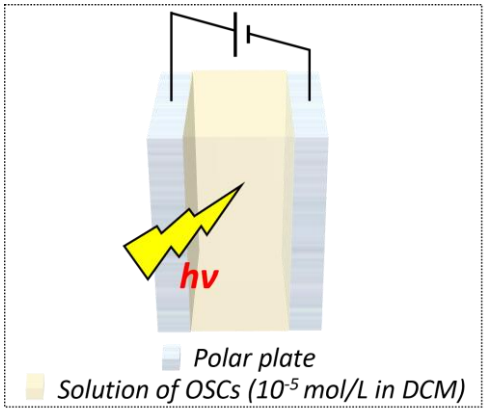

Fig. S20 Diagram of measurement method in PQ-4FP and PQ-4ClP solution.

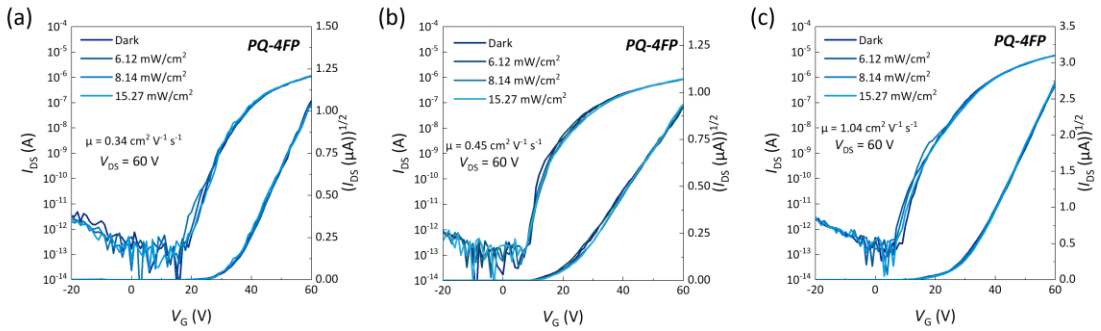

Fig. S21 Transfer curves and mobilities of PQ-4FP under dark and UV light irradiation conditions (385 nm) with different light power densities.

9. NMR spectra

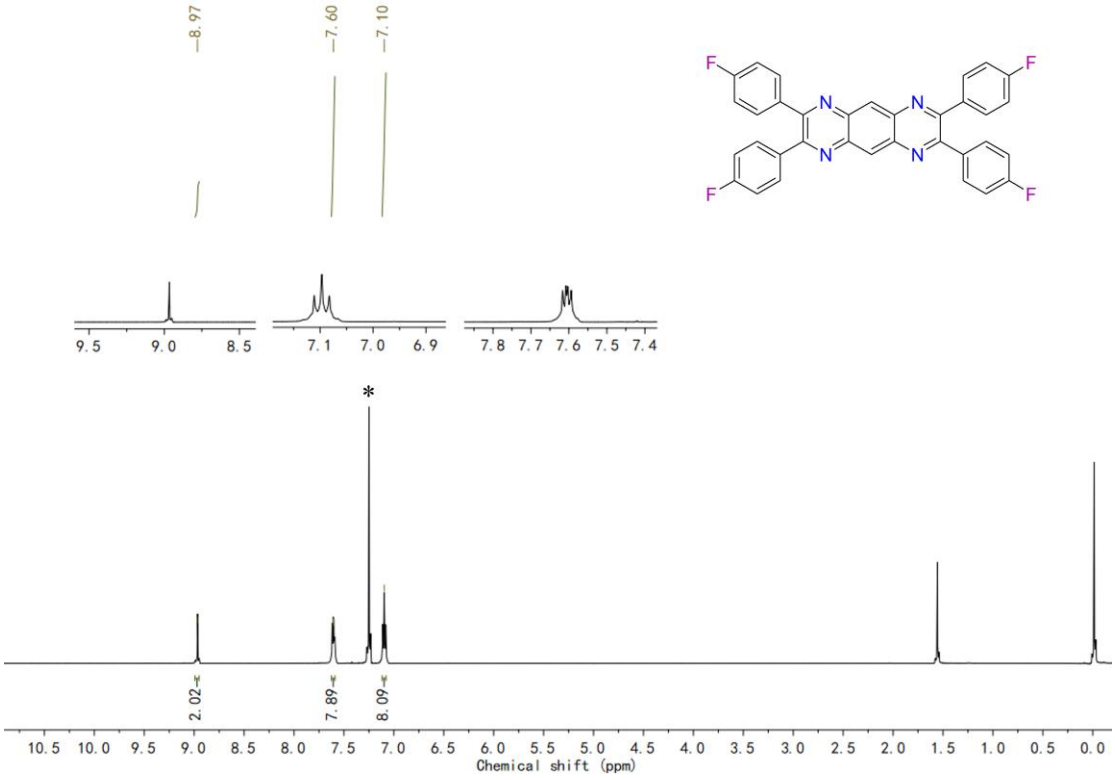

Fig. S22 ^{1}H NMR of PQ-4FP (ppm).

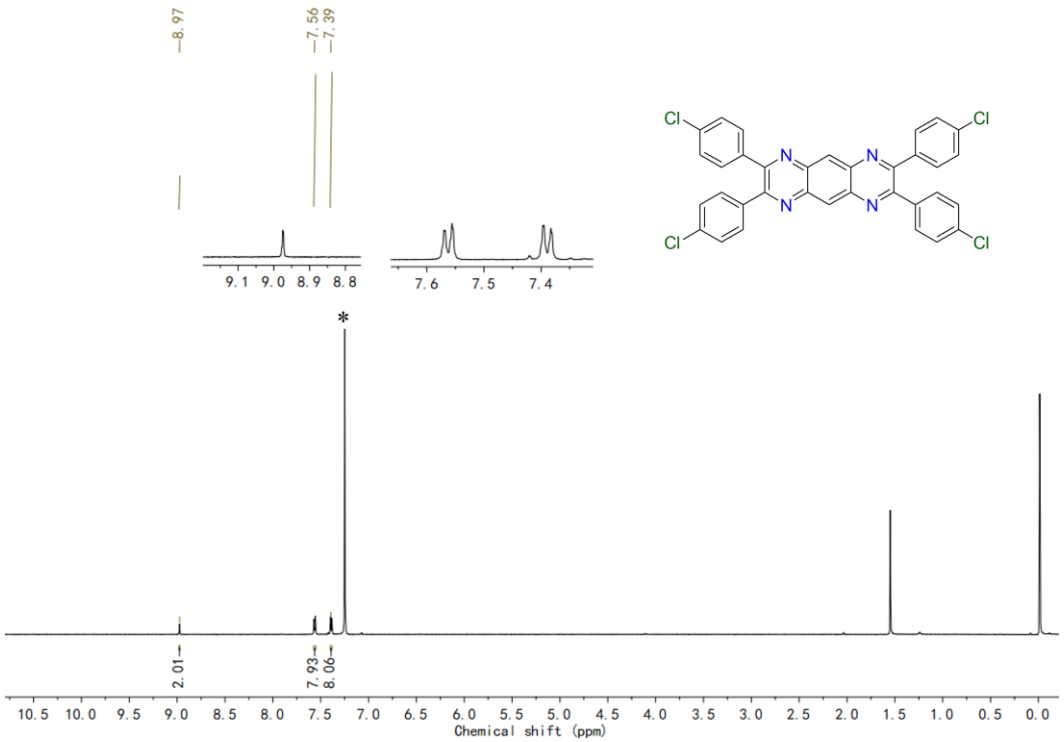

Fig. S23 ^{1}H NMR of PQ-4ClP (ppm).

10. HRMS

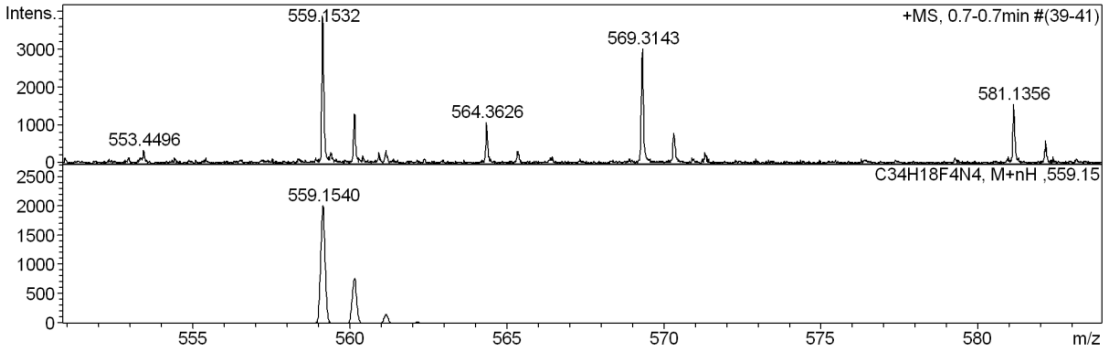

Fig. S24 HRMS spectra of PQ-4FP.

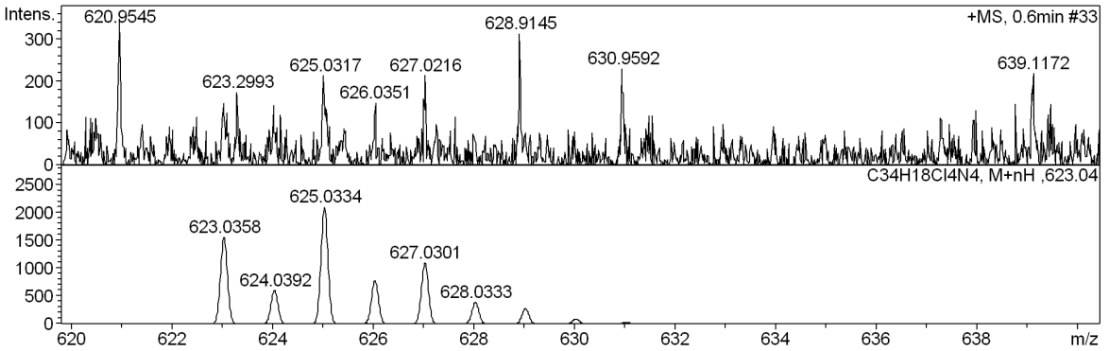

Fig. S25 HRMS spectra of PQ-4ClP.

11. References

1 M. J. Frisch, G. W. Trucks, H. B. Schlegel, G. E. Scuseria, M. A. Robb, J. R. Cheeseman, G. Scalmani, V. Barone, G. A. Petersson and H. Nakatsuji, *Gaussian 16, revision A.03*, Gaussian Inc., Wallingford, CT, 2016.